Available online at www.sciencedirect.com
ScienceDirect
Journal of Energy Chemistry 22(2013)876–882
JOURNAL OF ENERGY CHEMISTRY
www.elsevier.com/locate/jngc

Methane conversion into higher hydrocarbons with dielectric barrier discharge micro-plasma reactor

Baowei Wang*, Wenjuan Yan, Wenjie Ge, Xiaofei Duan

Key Laboratory for Green Chemical Technology of the Ministry of Education, School of Chemical Engineering and Technology, Tianjin University, Tianjin 300072, China

[Manuscript received February 3, 2013; revised March 12, 2013]

Abstract

We reported a coaxial, micro-dielectric barrier discharge (micro-DBD) reactor and a conventional DBD reactor for the direct conversion of methane into higher hydrocarbons at atmospheric pressure. The effects of input power, residence time, discharge gap and external electrode length were investigated for methane conversion and product selectivity. We found the conversion of methane in a micro-DBD reactor was higher than that in a conventional DBD reactor. And at an input power of 25.0 W, the conversion of methane and the total C_2+C_3 selectivity reached 25.10% and 80.27%, respectively, with a micro-DBD reactor of 0.4 mm discharge gap. Finally, a nonlinear multiple regression model was used to study the correlations between both methane conversion and product selectivity and various system variables. The calculated data were obtained using SPSS 12.0 software. The regression analysis illustrated the correlations between system variables and both methane conversion and product selectivity.

Key words

dielectric barrier discharge; hydrocarbons; methane; micro-reactor; plasma

1. Introduction

Methane is the primary component of natural gas and shale gas. In recent years, CH_4 has also become increasingly relevant in chemistry and industry, both as a source of H_2 and a raw material for producing other complex hydrocarbons. This conversion of CH_4, however, is a challenging problem because of the strong bond energy of C–H in methane [1]. Many researchers are trying to develop technology to overcome this problem [2−4]. Of the methods being developed, the use of non-thermal plasma is one of the most promising method. Non-thermal plasma is an effective tool to generate energetic electrons because it is not in thermodynamic equilibrium and can initiate a series of chemical processes, such as ionization, dissociation and excitation. Research teams have studied various discharge techniques for direct methane conversion, including corona discharge [5], spark discharge [6], microwave discharge [7], pulsed plasma [8], gliding arc discharge [9] and dielectric barrier discharge (DBD) [10−13].

DBD is commonly used in direct CH_4 conversion to industrially valuable chemicals and liquid fuels at atmospheric pressure because of its low cost and ease of use [14]. The primary drawbacks of using conventional DBD reactor for CH_4 conversion are lower levels of conversion, poor selectivity to desired hydrocarbons and higher energy cost.

A more favorable alternative is the micro-dielectric barrier discharge (micro-DBD) technique, in which the plasma is confined to critical dimensions below approximately 1 mm, with the energy density comparatively higher [15]. Micro-DBD technology has been widely used for chemical synthesis [16,17] and micro-chemical analysis [18]. Additionally, micro-DBD combines the advantages of non-thermal plasma with those of micro-reactors, offering better control of processing parameters for the selective synthesis of particular products. Recently, Ağiral et al. [17] reported a multi-phase flow, non-thermal plasma micro-DBD reactor for the partial oxidation of methane to liquid oxygenates at atmospheric pressure. Micro-DBD can improve both the one-pass conversion of methane and product selectivity, allowing liquid component selectivity to reach 25% due to the lower reaction temperature.

Although the conversion of methane could be enhanced by the presence of oxygen, which could also further oxidize the desired products produced in intermediate reaction steps. Therefore, in this study, only pure methane was fed into the electric discharge environment so the steady-state reaction behavior could be monitored in a non-oxidative environment.

* Corresponding author. Tel: +86-22-27402944; Fax: +86-22-87401818; E-mail: wangbw@tju.edu.cn
This work was supported by the National Natural Science Foundation of China (NSFC) under the grant of No. 21176175 and No. 20606023.

The micro-DBD reactor was used to convert methane into valuable products such as ethane, ethylene acetylene and propane. In order to compare a micro-DBD with the conventional DBD reactor for the conversion of methane, the conventional DBD with a discharge gap of 1.9 mm was also investigated, and the difference between micro-DBD and conventional DBD reactor was discussed. The effects of input power, discharge gap, residence time and external electrode length on methane conversion and hydrocarbon selectivity were investigated. Finally, we used a nonlinear multiple regression model to examine the correlation of methane conversion and product selectivity with the abovementioned system variables within appropriate ranges, and we discussed the reaction process.

2. Experimental

2.1. Experimental setup

The schematic diagram of the experimental setup is shown in Figure 1. The setup consisted of three parts: a micro-DBD reactor, a flow control device and a detection and analysis system. The micro-DBD reactor consisted of a quartz tube with wall thickness of 1 mm (inner diameter (r): 5.8 mm; length: 200 mm) which was equipped with an internal stainless steel electrode (various outer diameters (D) were used to alter the discharge gap). The external aluminum foil electrode was wrapped around the outside of the quartz tube. A thermocouple was attached to the outer wall of the quartz tube to measure the reactor wall temperature, located 5.0 mm above the ground electrode. The discharge was initiated when AC voltage sufficient power (CTP-2000, Nanjing Suman Electronic Company Limited) was applied between the two electrodes. The AC voltage applied in this study was 6.4−8.6 kV. The voltage and current waveforms were measured with an oscilloscope (DPO-2012, Tektronix) using a voltage probe (P6015A, Tektronix) and a current monitor (A622, Tektronix).

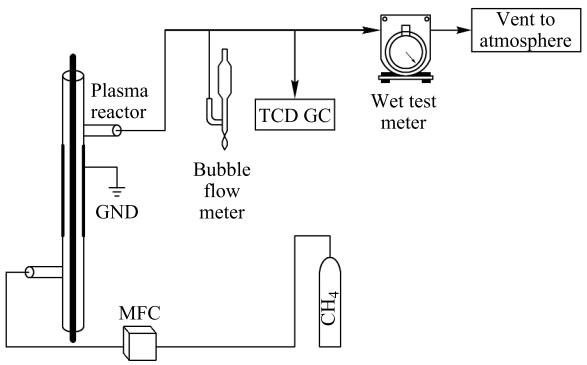

Figure 1. Schematic diagram of CH_4 conversion by micro-DBD reactor

2.2. Gas flow measurement and analytical system

Pure methane (99.9%) was introduced into the micro-DBD reactor. All the experiments were performed at atmospheric pressure. The feed gas flow rate was controlled by a set of mass flow controllers (MFCs) that were calibrated using a bubble flow meter. To check the outlet gas, the flow rate of effluent gas was measured with a bubble flow meter, while the cumulative flow rate of effluent gas was measured with a wet test meter during the experiment. The total gas flow rates were varied from 20 mL/min to 60 mL/min. In the following discussion, the compositions of outlet gases in all the experiments were analyzed continuously by gas chromatography (GC) for plasma reactions that were maintained for 10 min or longer unless otherwise specified. The GC, equipped with a thermal conductivity detector (TCD) and using He as the carrier gas, was able to detect H_2 and CH_4 with a TDX-01 column (2 m length×3 mm I.D.) and to detect C_2H_2+C_2H_4, C_2H_6 and C_3H_8+C_3H_6 with a Hevy Seep DB column. The concentrations of CH_4, C_2H_2+C_2H_4, C_2H_6 and C_3H_8 hydrocarbons were evaluated using the external standard analysis method.

The reactor weight (the sum weights of the quartz tube and the inner stainless electrode) was measured using an analytic balance (Mettler Toledo AL204). Carbon weight was determined as the difference between the reactor weights before and after the plasma reaction.

The evaluation of system performance, i.e. methane conversion and selectivity are formulated using the following equations:

$$X_{\mathrm{CH_4}}(\%) = \frac{(F^{\mathrm{in}}_{\mathrm{CH_4}} - F^{\mathrm{out}} \cdot C^{\mathrm{out}}_{\mathrm{CH_4}})}{F^{\mathrm{in}}_{\mathrm{CH_4}}} \times 100\% \qquad \text{(E1)}$$

where, $F^{\mathrm{in}}_{\mathrm{CH_4}}$ and F^{out} (mL/min) represent the flow rate of CH_4 at the inlet of the reactor and the flow rate of effluent gas at the outlet of the reactor, respectively; $C^{\mathrm{out}}_{\mathrm{CH_4}}$ represents the molar fraction of CH_4 in the effluent gas, as indicated by GC.

The selectivities to H_2 ($S_{\mathrm{H_2}}$) and hydrocarbons ($S_{\mathrm{C}_x\mathrm{H}_y}$) are calculated from the following equations:

$$S_{\mathrm{C}_x\mathrm{H}_y}(\%) = \frac{X \cdot F^{\mathrm{out}} \cdot C^{\mathrm{out}}_{\mathrm{C}_x\mathrm{H}_y}}{F^{\mathrm{in}}_{\mathrm{CH_4}} \cdot X_{\mathrm{CH_4}}} \times 100\% \qquad \text{(E2)}$$

$$S_{\mathrm{H_2}}(\%) = \frac{0.5 \cdot F^{\mathrm{out}} \cdot C^{\mathrm{out}}_{\mathrm{H_2}}}{F^{\mathrm{in}}_{\mathrm{CH_4}} \cdot X_{\mathrm{CH_4}}} \times 100\% \qquad \text{(E3)}$$

here, x and y represent carbon-atom number and hydrogen-atom number, respectively, in a resulting hydrocarbon molecule; $C^{\mathrm{out}}_{\mathrm{CH_4}}$ and $C^{\mathrm{out}}_{\mathrm{C}_x\mathrm{H}_y}$ represent the molar fractions of H_2 and hydrocarbons in the effluent gas, respectively, as indicated by GC.

The carbon deposition has an important role in the carbon balance. The carbon selectivity is defined as the following equation:

$$S_{\mathrm{C}}(\%) = \frac{m}{12 \times \text{moles of } \mathrm{CH_4} \text{ converted}} \times 100\% \qquad \text{(E4)}$$

where m (g) is the difference between the reactor weights before and after the plasma reaction.

Carbon balance is defined as the following equation, in which t (min) is the reaction time.

$$B_C(\%) = \frac{F^{out} \cdot t \cdot (x \cdot C^{out}_{C_xH_y} + C^{out}_{CH_4}) \times 100 + 316581 \cdot \quad m}{F^{in}_{CH_4} \cdot t} \tag{E5}$$

The residence time (s) were calculated as follows:

$$\tau = \frac{0.06 \times 3.14 \cdot d(r+D)L}{F^{in}_{CH_4}} \tag{E6}$$

here, d (mm) is the discharge gap, r (mm) is the inner diameter of quartz tube, D (mm) is the outer diameter of internal stainless steel electrode, and L (mm) is the length of the external electrode.

The specific energy input (*SEI*, kJ/L) in this study is defined as the total input power (P_{input}, W) divided by the total feed flow rate ($F^{in}_{CH_4}$, mL/min).

$$SEI = \frac{60 \times P_{input}}{F^{in}_{CH_4}} \tag{E7}$$

3. Results and discussion

3.1. Effect of residence time

The residence time was shown to be an important factor for a gas-phase reaction. Its influence on the conversion of methane and products selectivities was studied by changing the flow rate of methane. Figure 2 shows the conversion of methane and products selectivities as a function of residence time. The conversion of methane rapidly increased from 9.63% to 20.31% as the residence time increased. This rapid conversion occurred because during the DBD plasma process, the first step is the dissociation of the molecular species by electron collision, followed by the chemical reaction, initiated by the ionic and excited atomic or molecular species, which results in the synthesis of the desired species [19−21]. When the residence time of the reaction was prolonged, the probability of the effective collision between methane and other energetic radicals increased. Because of the micro-reactor geometry used in this experiment, the residence time was 4.11 s at a flow rate of 20.24 mL/min and 1.39 s at a flow rate of 59.75 mL/min. The *SEI* also increased from 25.75 kJ/mol to 72.33 kJ/mol with increasing residence time. This meant the average input energy per CH_4 molecule increased with increasing residence time which, in turn, increased the conversion of CH_4.

Figure 2 shows that the products selectivities changed with residence time in various ways. The selectivities of C_2H_6 and C_2H_2+C_2H_4 slightly changed from 48.79% to 44.81% and from 15.54% to 11.20%, respectively, as the residence time increased from 1.39 s to 4.11 s, while the selectivity of C_3 hydrocarbons slightly changed from 11.89% to 16.69%. The trends implied that C_3 was generated primarily by the coupling of C_1 and C_2 species. In the case of longer residence time, more neutral molecules were activated to C_1 and C_2 radicals, which were available for coupling to C_3 species, increasing C_3 selectivity. C_3 formation may be shown as follows (R1−R4):

Propane formation:

$$C_2H_5 \cdot + CH_3 \cdot \longrightarrow C_3H_8 \tag{R1}$$

$$C_2H_5 \cdot + CH_4 \longrightarrow C_3H_8 + H \cdot \tag{R2}$$

Propylene formation:

$$C_2H_4 + CH_2 \cdot \longrightarrow C_3H_6 \tag{R3}$$

$$C_2H_3 \cdot + CH_4 \longrightarrow C_3H_6 + H \cdot \tag{R4}$$

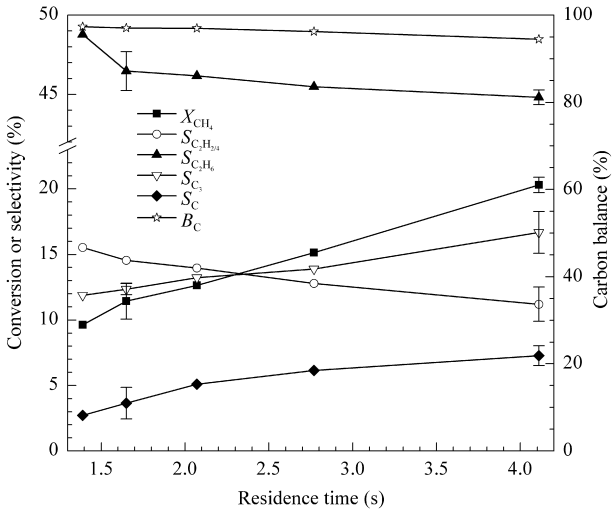

Figure 2. Effect of residence time on the conversion of CH_4 and products selectivities. Reaction conditions: input power = 25.0 W, discharge gap = 0.9 mm and external electrode length = 100.0 mm

3.2. Effect of input power

Figure 3 shows the effects of input power on the conversion of CH_4, applied voltage and current, *SEI*, products selectivities and carbon balance at a feed flow rate of 20.00±0.20 mL/min. The applied voltage and applied current increased from 6.6 kV to 8.0 kV and 1.7 A to 2.3 A, respectively, with an increase in input power from 10.4 W to 25.6 W, while *SEI* increased from 31.04 kJ/L to 76.27 kJ/L. These results indicated that the applied electric field was enhanced and the average input energy per methane molecule increased by increasing the input power. The conversion of methane rapidly increased from 7.46% to 20.52%. This result demonstrated that the input power had a powerful and positive effect on the conversion of methane. Increasing the input power to 30.4 W, however, methane conversion changed very little because of the highest applied current and voltage, which can destroy the reactor and made the plasma process unstable. At the input power of 30.4 W, the selectivity to carbon was 9.00%, which has a bad effect on plasma process.

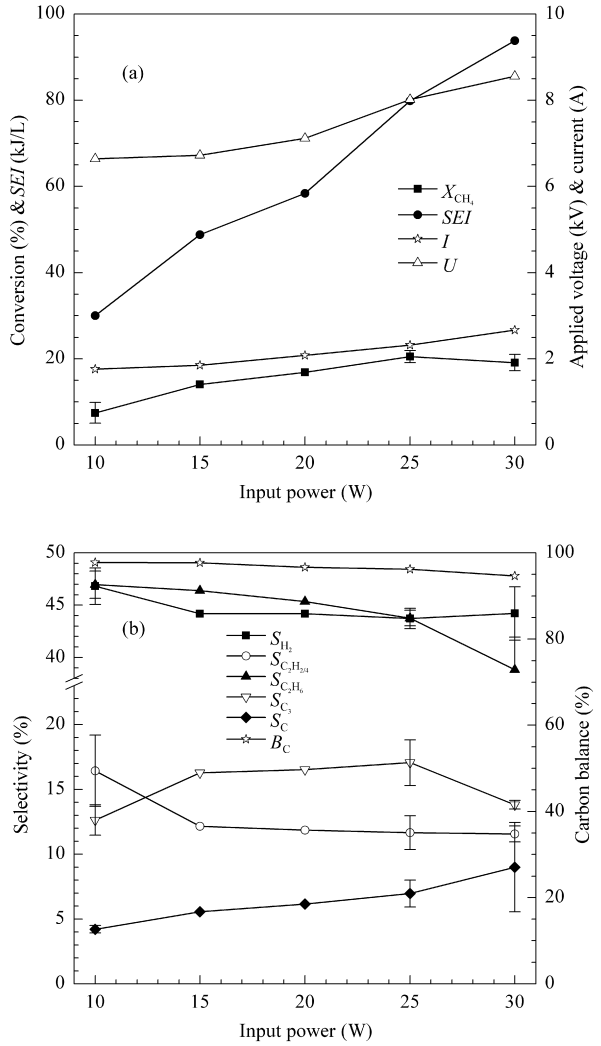

Figure 3. Effect of input power on (a) the conversion of CH_4, *SEI*, applied voltage, and applied current, and (b) the products selectivities. Reaction conditions: residence time $\sim$ 4.1 s, discharge gap = 0.9 mm and the external electrode length = 100.0 mm

In this experiment, C_2H_6 was the primary product, and C_2H_6 selectivity was approximately 46%. Based on thermodynamic calculations, the minimum energy requirements for the formation of ethylene and ethane were 202.59 kJ/mol and 67.53 kJ/mol, respectively, which means that more energy is required for the formation of ethylene than that for ethane [22]. In micro-DBD plasma used in this study, the energy per pulse was less than 1.3 mJ, and ethane was the major C_2 product because of short period ($<$52 μs) and low current pulses. The primary reaction processes for forming ethane are illustrated in Reactions R5 and R6.

$$CH_3\cdot + CH_3\cdot \longrightarrow C_2H_6 \quad \text{(R5)}$$

$$CH_4 + CH_3\cdot \longrightarrow C_2H_6 + H\cdot \quad \text{(R6)}$$

The selectivity to C_3 changed from 12.63% to 17.76% when the input power increased from 10.4 W to 25.6 W (Figure 3b). This phenomenon was the result of the dominant production of propane in the radical-radical reaction. In higher applied electric field, more C_2H_6 and CH_4 molecules were activated to $C_2H_5\cdot$ and $CH_3\cdot$, which contributed to the formation of propane.

3.3. Effect of external electrode length

The effect of external electrode length on the conversion of methane and products selectivities for a given residence time is illustrated in Figure 4. The applied current and voltage decreased with increasing external electrode length, although the "breakdown" voltage changed very little at a constant input power. When the external electrode length was increased from 100 mm to 200 mm, the conversion of methane decreased from 20.28% to 13.03% (Figure 4).

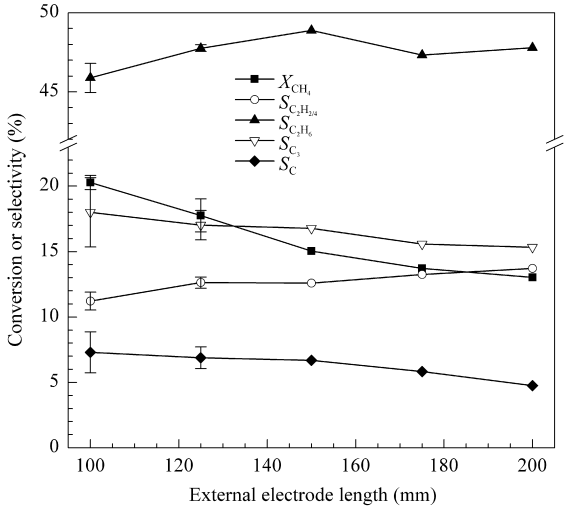

Figure 4. Effect of external electrode length on the conversion of CH_4 and products selectivities. Reaction conditions: input power = 25.0 W, discharge gap = 0.9 mm, residence time $\sim$ 4.1 s

This finding resulted from the fact that in a DBD reactor, more than half of the electrical energy is spent on heating the dielectric barrier [23]. In this experiment, the barrier volume increased from 2.13 cm^3 to 4.27 cm^3 when the external electrode length was increased from 100.0 mm to 200.0 mm, resulting in more energy being needed to heat the dielectric barrier for the same input power level. The surface area of the reactor increased from 24.49 cm^2 to 48.98 cm^2, increasing the radiator surfaces and dissipating more heat as well. Simultaneously, the applied voltage decreased from 8.0 kV to 6.5 kV and the current decreased from 2.3 A to 1.3 A. The applied electric field intensity decreased from 8.89 kV/mm to 7.22 kV/mm. These results indicated that the effective energy for plasma reaction decreased and the applied electric field became weaker, decreasing the conversion of methane. Additionally, in this experiment, *SEI* decreased from 75.89 kJ/L to 37.02 kJ/L, indicating that the average input energy per methane molecule decreased, which further contributed to a decrease of methane conversion.

To eliminate the influence of *SEI* on the conversion of methane, in the following experiment, we investigated

the effect of external electrode length on the conversion of methane at a fixed *SEI* (76.50±0.50 kJ/L). The conversion of CH_4 and products selectivities are shown in Figure 5. As the external electrode length was increased from 80.0 mm to 140.0 mm, the residence time increased from 3.34 s to 5.81 s. In general, for a given input power, longer residence time resulted in higher conversion of methane. However, in this experiment, the conversion of methane peaked at 100.0 mm and changed very little as the external electrode length was increased to 140.0 mm. The reason for this behavior was that as mentioned before, the barrier volume and the radiator surfaces increased with increasing external electrode length. More energy was needed to heat the dielectric barrier. For example, with an external electrode length of 140.0 mm (barrier volume of 2.99 cm^3), the applied voltage and current were 7.0 kV and 2.0 A. With an external electrode length of 100 mm (barrier volume of 2.13 cm^3), the applied voltage and current were 8.0 kV and 2.3 A. The applied voltage and current for an external electrode length of 140 mm was weaker than that for an external electrode length of 100 mm, which had a negative effect on methane conversion. The conversion of methane reached a maximum of 20.34%, corresponding to an external electrode length of 100.0 mm, and did not change as the external electrode length was increased beyond 100.0 mm.

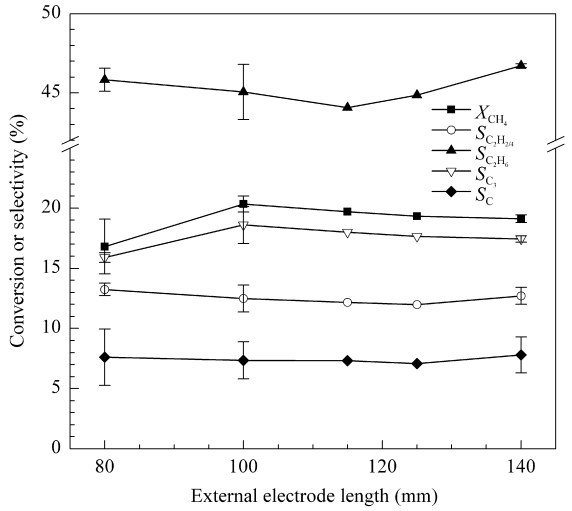

Figure 5. Effect of external electrode length on the conversion of CH_4 and products selectivities. Reaction conditions: input power = 25.0 W and discharge gap = 0.9 mm

From Figures 4 and 5, we determined that the external electrode length was not a significant contributing factor in the determination of products selectivities; C_2H_6 selectivity was approximately 46%, C_2H_2+C_2H_4 selectivity was approximately 12% and C_3H_8 selectivity was approximately 17%.

3.4. Effect of discharge gap

Figure 6 shows the characteristics of the conversion of methane in a DBD plasma reactor at various discharge gaps. The discharge gap of 0.4 mm and 0.9 mm was investigated in this experiment. In order to compare our micro-DBD reactor with the conventional DBD for the conversion of methane, the conventional DBD with a discharge gap of 1.9 mm was also investigated.

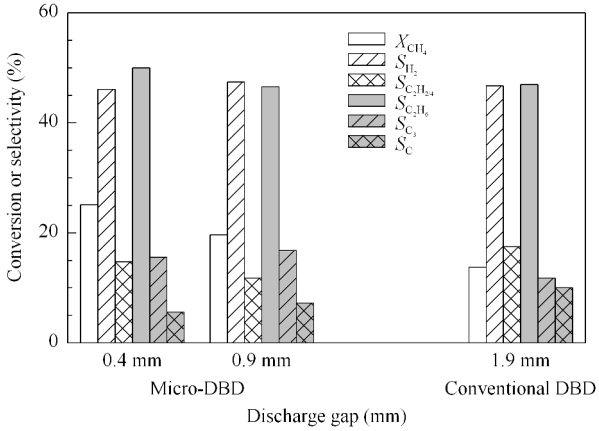

Figure 6. Effect of discharge gap on the conversion of CH_4 and products selectivities. Reaction conditions: input power = 25.0 W, residence time ∼ 4.1 s and external electrode length = 100.0 mm

It is known that DBD is characterized by a diffuse discharge at atmospheric pressure and is also characterized by many micro-discharge channels. The number of micro-discharge channels is proportional to the voltage applied to the electrodes [14]. In this experiment, the applied voltage and current remained nearly constant at 8.0 kV and 2.2 A for the discharge gap of 0.4 mm, 0.9 mm and 1.9 mm. Consequently, the number of micro-discharges did not change significantly. However, *SEI* was 149.2 kJ/L, 75.9 kJ/L and 44.4 kJ/L, which had a positive effect on the conversion of methane. In this experiment, the conversion of methane was 25.10%, 20.01% and 13.76% at a discharge gap of 0.4 mm, 0.9 mm and 1.9 mm.

In the following experiments, the influence of discharge gap was investigated for the case of a feed flow rate of 20.00±0.20 mL/min and input power of 25.0 W (the *SEI* remained constant at 76.40±0.40 kJ/L). The applied voltage and current did not change significantly. At a discharge gap of 0.4 mm, 0.9 mm and 1.9 mm, the conversion of methane was 20.22%, 20.30% and 15.80%, respectively (Figure 7). These results indicated that the conversion of methane was higher when the discharge gap was less than 1 mm. Although the longest residence time (6.94 s) coincided with a discharge gap of 1.9 mm, the conversion of methane was the lowest. This fact was the result of low plasma density and applied electric field intensity, leading to the decrease in conversion of methane. The products selectivities in the experiment did not show apparent change (Figure 7).

The selectivity to C was investigated for the case of a residence time of 4.1 s (Figure 6) and for the case of a feed flow rate of 20.00 mL/min (Figure 7). For both case the selectivity to C in a conventional DBD reactor was the highest. In fact, the carbon deposition reduces the number of discharge streamers and limits the number of energetic electrons that interact with the feed gases in the reaction zone, thereby lowering

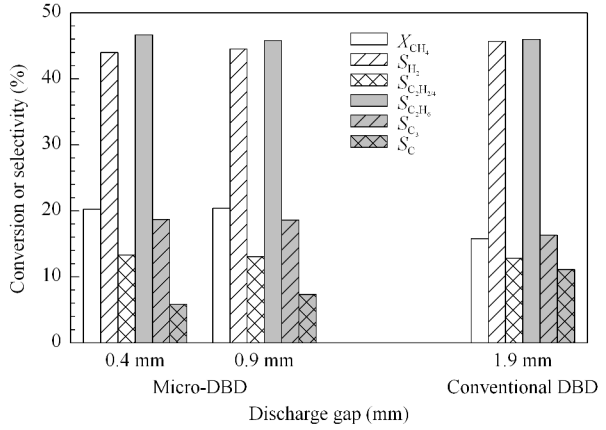

Figure 7. Effect of discharge gap on the conversion of CH_4 and products selectivities. Reaction conditions: input power = 25.0 W and external electrode length = 100.0 mm

the conversion of methane. While in a micro-DBD reactor, the density of hydrogen radicals was higher for the case of a small discharge gap, which resulted from the increased conversion of methane and the smaller discharge space. The hydrogen radicals played an essential role in the removal of undesired carbon deposits (R7, R8) [7]. So the selectivity to C was lower and the conversion of methane was higher in a micro-DBD reactor.

$$C(s) + H\cdot = CH\cdot \quad \text{(R7)}$$

$$CH(s) + H\cdot = CH_2\cdot \quad \text{(R8)}$$

It is noteworthy that the energy consumption for converting methane was 10.6 MJ/mol, 8.5 MJ/mol and 8.4 MJ/mol for the discharge gap of 1.9 mm, 0.9 mm and 0.4mm, respectively. It meant that the energy consumption for converting methane was higher in a conventional DBD reactor than that in a micro-DBD reactor.

Interestingly, the wall temperature was 448 K, 463 K and 523 K for the discharge gaps of 0.4 mm, 0.9 mm and 1.9 mm, respectively (25.0 W). In this experiment, the input power was held constant, but during the plasma reaction, the wall temperature value was lower for a smaller discharge gap. This implied that more energy was used for the plasma reaction and less for heating the reactor and heat loss. Due to low temperature and small discharge gap, the amount of energy that was wasted was reduced, and the heat transfer performance and plasma reaction stability were improved. Therefore, the energy for methane conversion reaction increased, and the conversion of methane was higher for a small discharge gap.

3.5. Correlations between system variables

Nonlinear multiple regression analysis was used to analyze the data in this study. The data regression over system variables to correlate methane conversion and C_2 or C_3 selectivity has been done by the following model equations. SPSS 12.0 software was used for the data regression.

$$X_{CH_4} = \alpha + \alpha_1 x_1 + \alpha_2 x_2 + \alpha_3 x_3 + \alpha_4 x_4 + \alpha_{11} x_{11}^2 + \alpha_{22} x_{22}^2 + \alpha_{33} x_{33}^2 + \alpha_{44} x_{44}^2 + \alpha_{12} x_1 x_2 + \alpha_{13} x_1 x_3 + \alpha_{14} x_1 x_4 + \alpha_{23} x_2 x_3 + \alpha_{24} x_2 x_4 + \alpha_{34} x_3 x_4 \quad \text{(E8)}$$

$$S_{C_2H_6} = \beta + \beta_1 x_1 + \beta_2 x_2 + \beta_3 x_3 + \beta_4 x_4 + \beta_{11} x_{11}^2 + \beta_{22} x_{22}^2 + \beta_{33} x_{33}^2 + \beta_{44} x_{44}^2 + \beta_{12} x_1 x_2 + \beta_{13} x_1 x_3 + \beta_{14} x_1 x_4 + \beta_{23} x_2 x_3 + \beta_{24} x_2 x_4 + \beta_{34} x_3 x_4 \quad \text{(E9)}$$

$$S_{C_3} = \gamma + \gamma_1 x_1 + \gamma_2 x_2 + \gamma_3 x_3 + \gamma_4 x_4 + \gamma_{11} x_{11}^2 + \gamma_{22} x_{22}^2 + \gamma_{33} x_{33}^2 + \gamma_{44} x_{44}^2 + \gamma_{12} x_1 x_2 + \gamma_{13} x_1 x_3 + \gamma_{14} x_1 x_4 + \gamma_{23} x_2 x_3 + \gamma_{24} x_2 x_4 + \gamma_{34} x_3 x_4 \quad \text{(E10)}$$

here, X_{CH_4}, $S_{C_2H_6}$, S_{C_3}, x_1, x_2, x_3 and x_4 are the conversion of methane, ethane selectivity, C_3 selectivity, discharge gap, residence time, external electrode length and input power, respectively; the terms $\alpha_{ij}x_ix_j$, $\beta_{ij}x_ix_j$ and $\gamma_{ij}x_ix_j$ represent the correlation effects between two variables x_i and x_j in the model. The three sets of model parameters were obtained to correlate the conversion of methane and products selectivities. The calculated model parameters are given in Table 1.

SPSS 12.0 software was also used for the correlativity analysis between X_{CH_4}, $S_{C_2H_6}$, S_{C_3} and x_1, x_2, x_3, x_4. The calculated data have been given in Table 2.

Table 2 shows that discharge gap had a negative effect on the conversion of methane, while residence time and input power had a significantly positive effect on the conversion of methane. This result can also be explained by Table 1 (α_1<0, α_2 and α_4>0). The interactions between discharge gap, residence time and input power had positive effects on the conversion of methane (α_{12}, α_{14}>0).

Table 1. Calculated values for parameters in model Equations (8)–(10)

α	α_1	α_2	α_3	α_4	α_{11}	α_{22}	α_{33}	α_{44}	α_{12}	α_{13}	α_{14}	α_{23}	α_{24}	α_{34}
10.20	−36.01	5.12	−0.17	2.05	3.68	−0.43	0.0001	−0.04	0.69	0.10	0.28	−0.01	0.04	−0.004
β	β_1	β_2	β_3	β_4	β_{11}	β_{22}	β_{33}	β_{44}	β_{12}	β_{13}	β_{14}	β_{23}	β_{24}	β_{34}
12.74	60.06	−13.08	0.20	1.90	−4.36	0.73	−0.001	−0.08	−4.02	−0.21	−0.38	0.05	0.30	0.004
γ	γ_1	γ_2	γ_3	γ_4	γ_{11}	γ_{22}	γ_{33}	γ_{44}	γ_{12}	γ_{13}	γ_{14}	γ_{23}	γ_{24}	γ_{34}
−71.19	95.84	0.95	0.59	0.48	3.15	1.10	−0.001	−0.02	−5.91	−0.40	−1.79	−0.07	0.29	0.01

Residence time had a significant effect on C_3 selectivity (Table 2). Generally, the large residence time encouraged C_3 formation ($\gamma_2>0$). However, the residence time had a negative effect on C_2H_6 selectivity (Table 2). The interaction between discharge gap, residence time, input power, and external electrode length also had negative effects on C_2H_6 formation ($\beta_{12}<0$, $\beta_{13}<0$, $\beta_{14}<0$).

Table 2. Correlativity analysis between X_{CH_4}, $S_{C_2H_6}$, S_{C_3} and x_1, x_2, x_3, x_4

	x_1	x_2	x_3	x_4
X_{CH_4}	−0.549[a]	+0.573[a]	−0.258	+0.606[a]
$S_{C_2H_6}$	+0.318	−0.207	+0.247	−0.232
S_{C_3}	+0.024	+0.412[b]	+0.324	−0.193

[a] x has a very significant effect on X_{CH_4}, $S_{C_2H_6}$ and S_{C_3}; [b] x has a marked effect on X_{CH_4}, $S_{C_2H_6}$ and S_{C_3}; "−" have a negative effect; "+" have an positive effect

MatLab 2011 software was used for constraint optimization for the correlation of Equation (8), subject to studied variables, which calculated the maximum value for the conversion of methane to be approximately 36.50%, corresponding to a discharge gap of 0.4 mm, a residence time of 4.00 s, an external electrode length of 100 mm and an input power of 27.7 W. Both the experimental results and predicted values implied that a small discharge gap and a long residence time encouraged the conversion of methane.

Applying the same procedure to Equations (10) and (11), the maximum value of 58.9% was calculated for C_2H_6 selectivity, corresponding to a discharge gap of 0.9 mm, a residence time of 1.00 s, an external electrode length of 100 mm and an input power of 13.79 W. Similarly, the calculated maximum value of 25% for C_3 selectivity corresponded to a discharge gap of 0.9 mm, a residence time of 2.08 s, an external electrode length of 200 mm and an input power of 30 W. This can be argued that for C_2 and C_3 hydrocarbons production we need fine adjusting to the system variables.

4. Conclusions

The newly developed non-thermal micro-DBD reactor enabled a single-step, selective synthesis of higher hydrocarbons at low temperatures. The micro-DBD reactor has great promise for direct synthesis of higher hydrocarbons from methane. The conversion of methane was higher with microplasma than that with conventional DBD reactor. The input power had a positive and significant effect on the conversion of CH_4 but a weak effect on product selectivity. C_2 selectivity decreased smoothly as the residence time was increased. C_3 selectivity increased and C selectivity decreased as the discharge gap was decreased. A longer residence time had a positive effect on C_3 formation. Moreover, the stability of the reaction was improved with the use of a micro-reactor due to the lower temperature.

The regression analysis revealed that the input power and residence time had positive effects on the conversion of CH_4, but larger discharge gap had negative effects. The residence time had a significant effect on C_3 selectivity. The interactions between the discharge gap, residence time, and input power had positive effects on the conversion of CH_4, but had negative effects on C_2H_6 selectivity.

Acknowledgements

Financial supports from the National Natural Science Foundation of China (NSFC) under the grant of No. 21176175 and No. 20606023 are acknowledged.

References

[1] Indarto A, Choi J W, Lee H, Song H K. *Energy*, 2006, 31(14): 2986
[2] Tao X M, Bai M G, Li X, Long H L, Shang S Y, Yin Y X, Dai X Y. *Prog Energy Combust Sci*, 2011, 37(2): 113
[3] Indarto A, Yang D R, Palgunadi J, Choi J W, Lee H, Song H K. *Chem Eng Process*, 2008, 47(5): 780
[4] Chen L, Zhang X W, Huang L, Lei L C. *Chem Eng Process*, 2009, 48(8): 1333
[5] Zhang X L, Dai B, Zhu A M, Gong W M, Liu C H. *Catal Today*, 2002, 72(3-4): 223
[6] Li X S, Zhu B, Shi C, Xu Y, Zhu A M. *AICHE J*, 2011, 57(10): 2854
[7] Zhang J Q, Yang Y J, Zhang J S, Liu Q, Tan K R. *Energy Fuels*, 2002, 16(3): 687
[8] Yao S L, Nakayama A, Suzuki E. *AICHE J*, 2001, 47(2): 413
[9] Rueangjitt N, Sreethawong T, Chavadej S, Sekiguchi H. *Plasma Chem Plasma Process*, 2011, 31(4): 517
[10] Bai M D, Zhang Z T, Bai M D, Bai X Y, Gao H H. *Plasma Chem Plasma Process*, 2008, 28(4): 405
[11] Wang Q, Yan B H, Jin Y, Cheng Y. *Plasma Chem Plasma Process*, 2009, 29(3): 217
[12] Pinhao N R, Janeco A, Branco J B. *Plasma Chem Plasma Process*, 2011, 31(3): 427
[13] Gallon H J, Tu X, Whitehead J C. *Plasma Process Polym*, 2012, 9(1): 90
[14] Kogelschatz U. *Plasma Chem Plasma Process*, 2003, 23(1): 1
[15] Iza F, Kim G J, Lee S M, Lee J K, Walsh J L, Zhang Y T, Kong M G. *Plasma Process Polym*, 2008, 5(4): 322
[16] Lindner P J, Besser R S. *Chem Eng Technol*, 2012, 35(7): 1249
[17] Ağıral A, Nozaki T, Nakase M, Yuzawa S, Okazaki K, Gardeniers J G E. *Chem Eng J*, 2011, 167(2): 560
[18] Zhu Z L, Chan G C Y, Ray S J, Zhang X R, Hieftje G M. *Anal Chem*, 2008, 80(22): 8622
[19] Istadi, Amin N A S. *Fuel*, 2006, 85(5-6): 577
[20] Lieberman M A, Lichtenberg A J. Principles of Plasma Discharges and Materials Processing. 2nd Ed. New York: John Wiley & Sons, 2005
[21] Kogelschatz U. *Plasma Chem Plasma Process*, 2003, 23(1): 1
[22] Li X S, Zhu A M, Wang K J, Xu Y, Song Z M. *Catal Today* 2004, 98(4): 617
[23] Hammer T, Kappes T, Baldauf M. *Catal Today*, 2004, 89(1-2): 5